

Ferromagnetism in Carbon doped Zinc Oxide Systems

B. J. Nagare*

Department of Physics, University of Mumbai, Santacruz (East), Mumbai-400 098, India.

Sajeev Chacko[†] and D. G. Kanhere[‡]

*Department of Physics and Center for Modeling and Simulation,
University of Pune, Ganeshkhind, Pune - 411 007, India.*

We report spin polarized density functional calculations of ferromagnetic properties of a series of ZnO clusters and solid containing one or two substitutional carbon impurities. We analyze the eigen value spectra, spin densities and molecular orbitals, and induced magnetic moments for ZnC, Zn₂C, Zn₂OC, carbon substituted clusters Zn_nO_n (n=3–10, 12) and ZnO solid. The results show that the doping induces magnetic moment of the $\sim 2 \mu_B$ in all the cases. All the systems with two carbon impurities show ferromagnetic interaction except when the carbon atoms share the same Zn atom as the nearest neighbor. This ferromagnetic interaction is predominantly mediated via π bonds in ring structures and through π and σ bonds in three dimensional structure. The calculations also show that the interaction is significantly enhanced in solid, bringing out the role of dimensionality of Zn-O network connecting two carbon atoms.

PACS numbers: 36.40.-c, 71.15.Mb, 75.50.Pp

I. INTRODUCTION

Dilute magnetic semiconductors (DMS) are a focus of much attention due to their potential application as spintronics material. These materials, apart from having a desirable band gap can exhibit room temperature ferromagnetism (RTF) upon doping by suitable impurities. Several oxides like TiO₂, SnO₂, In₂O₃, HfO₂ and more popular ZnO have been investigated and have been found to show ferromagnetism when doped with transition metal impurities.^{1,2,3,4,5} Amongst these, ZnO is preferred because of many attractive features. It has a wide band gap of 3.37 eV, suitable for applications with short wavelength light, a large exciton binding energy, a low lasing threshold, and is transparent to visible light.

There are a number of theoretical and experimental studies reported on ZnO yielding a variety of data on magnetic behavior. The data has raised many issues and at times, controversies. The density functional calculations show that doping by Cu produces half metallic ferromagnet⁶, the prediction has been verified experimentally.⁷ Co doping has generated much controversy about the origin of magnetism. Cobalt doped ZnO is reported to have high Curie temperature (TC) of up to 700 K. A robust ferromagnetic state is predicted at the Oxygen surface even in the absence of magnetic atoms.^{8,9} If Mn or Co is doped in films of ZnO, ferromagnetic behavior has been observed in both insulating and metallic films, but not when the carrier density is intermediate.¹⁰

Recently, non magnetic impurities have been shown to induce ferromagnetic behavior. Vacancy-induced magnetism in ZnO thin films and nano wires have been reported on the basis of density functional investigations.¹¹ In fact, defects of several types like vacancy at Zn site, oxygen surface, interstitial edges in nano ribbons¹² etc. have been reported to be inducing magnetic interactions. Recently, carbon doped ZnO has been shown to exhibit

ferromagnetic behavior with Curie temperature around room temperature.¹³ The experiment has been performed with two levels of doping, 1 % and 2.5 %. The spin density functional theory (SDFT) results show that the magnetism is due to ZnC system. The magnetic moment per carbon atom decreases slightly for the higher concentration from 2-3 μ_B to 1.5-2.5 μ_B . There are several unclear issues: the origin of magnetic moment on carbon site, the role of Zn and oxygen, the nature of the long range interaction between the two carbon sites, the role of oxygen-Zn network connecting the two sites. In order to gain some insight in to some of these issues, we have carried out a systematic density functional investigations on a series of systems, beginning with ZnC molecule. We have investigated the evolution of magnetic moments and magnetic interaction in ZnC, Zn₂C, Zn₂OC, Zn₂C₂ and then in a series of clusters Zn_nO_n (n=3–12) with a single and double carbon substitution. Finally we examine ZnO solid with a large unit cell of 72 atoms. We bring out the role of exchange splitting in Carbon atom, hybridization of Carbon p orbitals with Zn, the role of oxygen-Zn network, especially the role of dimensionality in stabilizing magnetic interactions.

II. COMPUTATIONAL METHOD

The calculations have been performed using SDFT with ultra soft pseudopotential and plane wave basis.^{14,15} We have used two different codes namely CASTEP¹⁵ and VASP.¹⁶ In all the cases, we have used generalized gradient approximation (GGA) given by Perdew-Burke-Ernzerhof (PBE).¹⁷ For clusters we have used supercells having lengths $\sim 15-30 \text{ \AA}$. The energy cut-off for the plane wave basis was chosen to 300 eV. The structures were considered to be converged when the force on each ion was less than $\sim 0.05 \text{ eV/\AA}$ with a maximum dis-

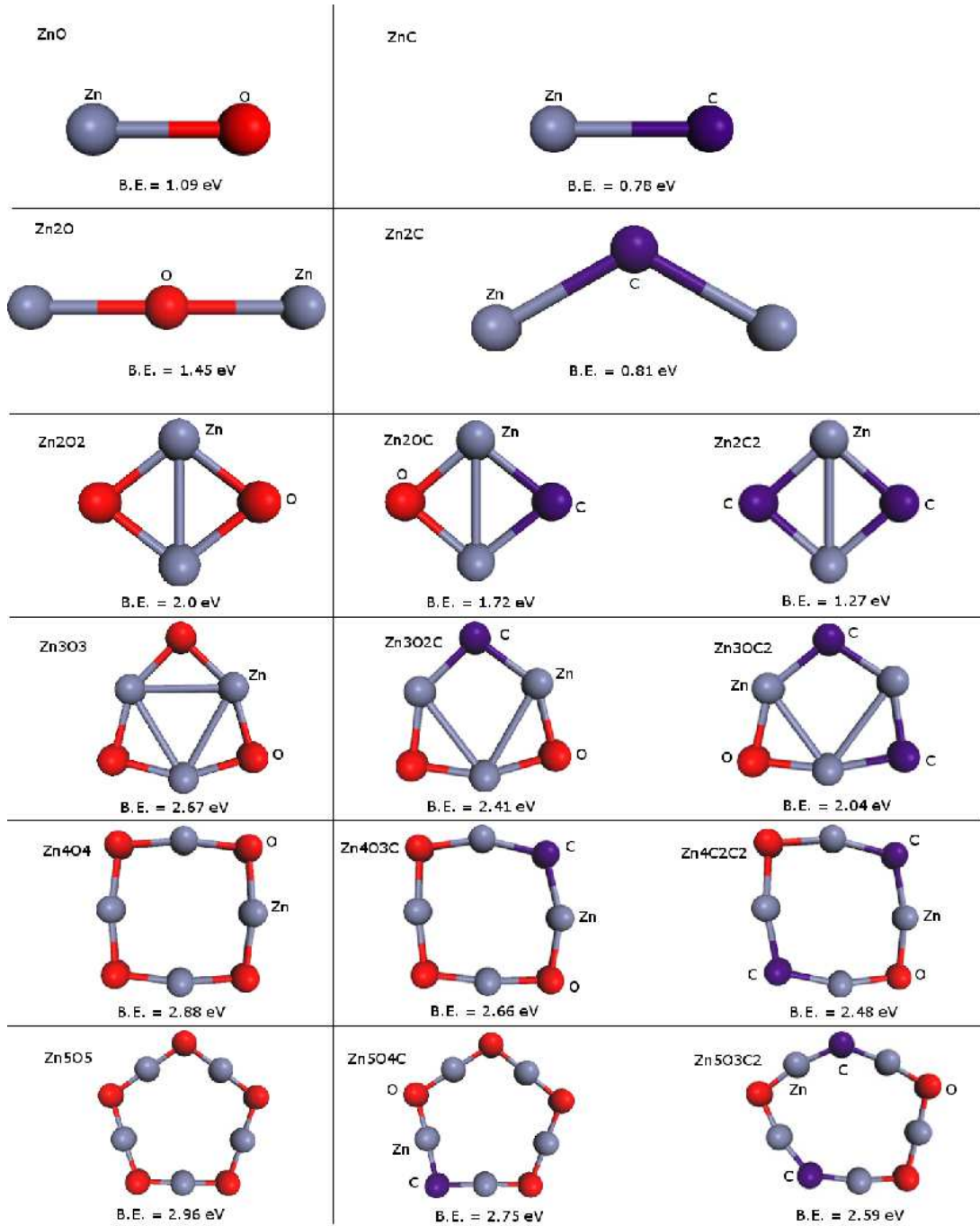


FIG. 1: Optimized ground state geometries of C-doped $(\text{ZnO})_n$ ($n=1-5$) clusters. The binding energy per atom (E_b) in eV is also shown. The oxygen atoms are indicated by red color (online) whereas substituted carbon is marked by C. The second and third column shows structures with single and double carbon substitution respectively.

placement of $\sim 0.002 \text{ \AA}$ and a convergence in the total energy of about $2 \times 10^{-6} \text{ eV/atom}$. In all the cases, the geometries of all the lowest energy structure are in good agreement with results of Matxain et. al.¹⁸ To study the magnetic properties of C-doped $(\text{ZnO})_n$ clusters, carbon atoms were doped substitutionally at various O-sites. The C-doped clusters were also optimized with the same set of parameters as used for $(\text{ZnO})_n$ clusters.

We have verified the accuracy of our model on ZnO molecule and ZnO solid. We find a bond length of 1.736 \AA and a binding energy 1.79 eV for ZnO molecule. The previous studies¹⁹ also report a bond length between $1.71-1.75 \text{ \AA}$. We also calculate the binding energy of the ZnO solid in the wurtzite structure. The calculated binding energy of 7.23 eV per ZnO unit agrees well with the experimental binding energy of 7.52 eV per ZnO as re-

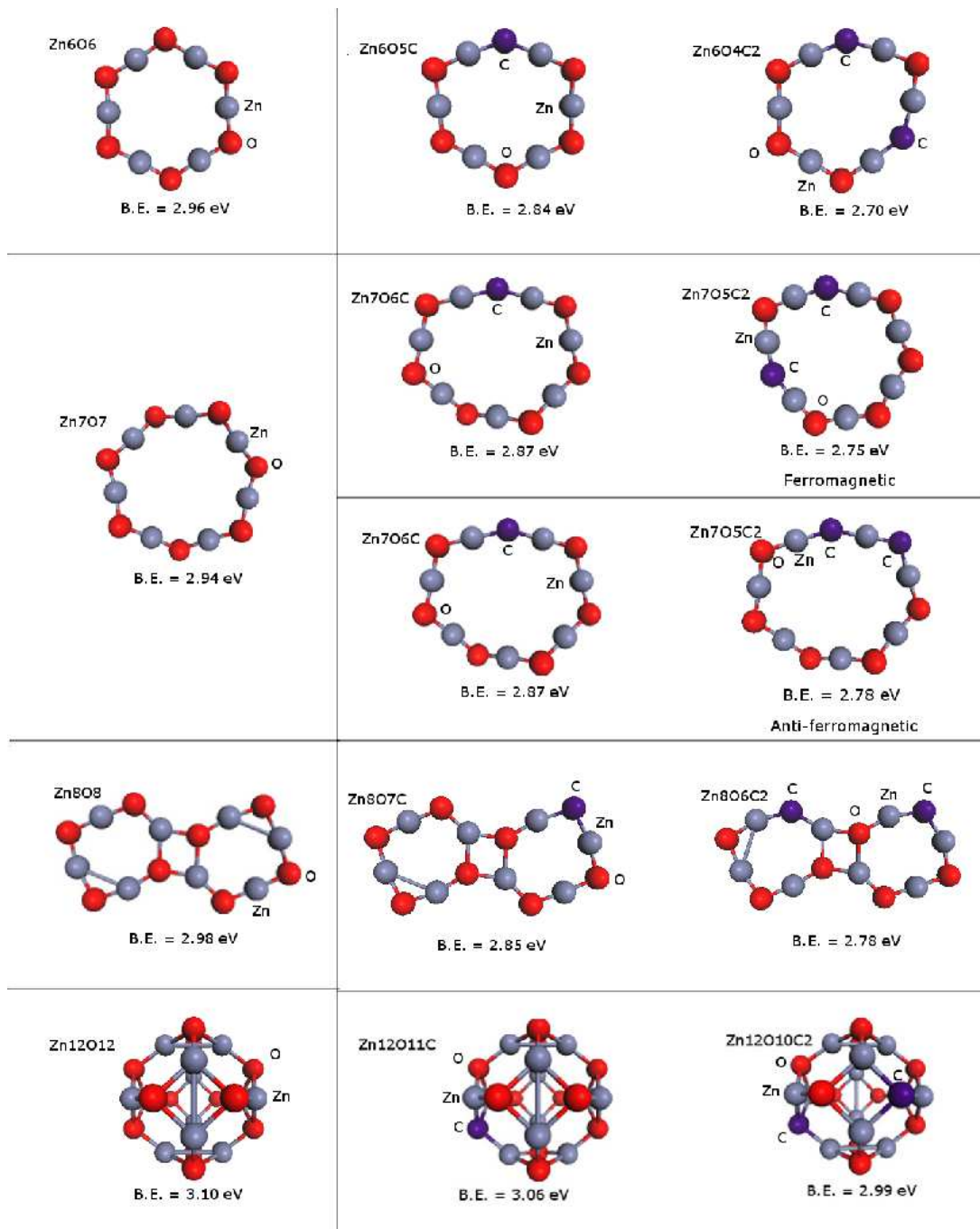


FIG. 2: Optimized ground state geometries of C-doped $(\text{ZnO})_n$ ($n=6-8, 12$) clusters. The binding energy per atom (E_b) in eV is also shown. The oxygen atoms are indicated by red color (online) whereas substituted carbon is marked by C. The second and third column shows structures with single and double carbon substitution respectively.

ported by Jaffe et.al.²⁰

In order to understand the basic mechanism of ferromagnetic origin and evolutionary trends, we have performed the calculations on series of clusters namely; ZnC , Zn_2C , $(\text{ZnO})_n$ and the substitutionally doped $\text{Zn}_n\text{O}_{n-m}\text{C}_m$ clusters with $n = 2 - 10, 12$ and $m = 1 - 2$ as well as on ZnO solid. In each of the cases, we substitute either one or two carbon atoms at O-sites.

In next section, we present and discuss our results.

III. RESULTS AND DISCUSSIONS

It is most fruitful to examine the electronic structure and systematics of magnetic properties of some important motifs in zinc oxide solid. When the carbon atom is

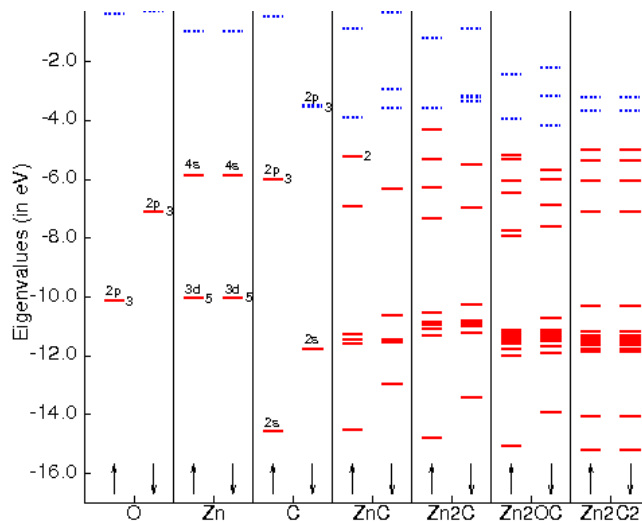


FIG. 3: The Eigenvalue spectra for some clusters. In each of the cases the left column is for up and right column is for down electrons. The unoccupied levels are shown by dotted lines. The numbers near the line shows degeneracy.

substitutionally doped at O-site in the bulk zinc oxide, it has zinc atom as the first nearest neighbor and oxygen atom as the second nearest neighbor. Therefore, we begin by examining the magnetism and the electronic structure of ZnC , Zn_2C , Zn_2OC , and Zn_2C_2 clusters. We have also calculated the electronic structure and the magnetic properties of ring structures of Zn_nO_n cluster ($n=3-8$) and $\text{Zn}_9\text{O}_9-\text{Zn}_{12}\text{O}_{12}$ which form three dimensional structures. The results are also presented for bulk zinc oxide by using large unit cell with 72 atoms. The optimized ground state geometries of these ZnO systems are shown in figure 1 and 2. It can be seen that the substitutional doping by carbon atoms has a small effect on the geometries of the hosts with exception of Zn_2O .

In table 1, we summarize the results of all C-doped clusters. The table shows the magnetic moments per site, the exchange energy E_J calculated as $E_{FM}-E_{AFM}$ (wherever appropriate) where, E_{FM} and E_{AFM} are the total energies of ferromagnetic and antiferromagnetic state respectively, the nature of magnetic ground state and nature of ground state geometries of C-doped clusters. A number of features can be discerned from table 1. 1. A majority of doubly doped $(\text{ZnO})_n$ clusters turn out to be ferromagnetic with magnetic moment of $\sim 2 \mu_B$ per carbon atom. 2. Whenever the same zinc atom is the nearest neighbor to both the carbon atoms, the ground state is antiferromagnetic. This is the case for Zn_2C_2 , Zn_3OC_2 and in other clusters when the carbon atoms are substituted on both sides of zinc atom. 3. It turns out that $\sim 80-90\%$ magnetic moment is localized on carbon sites with small but significant induced magnetic moment on oxygen and zinc sites (see figure 5 and the discussion). This is true for all singly and doubly substituted clusters irrespective of the placement of carbon atoms. 4. A

remarkable observation is that the exchange energy (E_J) is sensitive to the dimensionality of clusters and is highest for three dimensional clusters. Thus, the number of paths connecting two carbon atoms via zinc-oxygen network is a significant factor favouring the ferromagnetic coupling. In a sense this also brings out the role of oxygen in establishing the ferromagnetic interaction. We elaborate on this point in the discussion below.

In order to elucidate the origin of magnetism, we examine the eigenvalue spectra (figure 3) and the nature of molecular orbitals for ZnC , Zn_2C , Zn_2OC and Zn_2C_2 along with atomic Zn, O, and C which are shown in figure 4. We use the nomenclature alpha homo and beta homo to denote the highest occupied molecular orbitals for up spin and down spin respectively. In figure 3, we show the eigenvalue spectra for up spin (left part) and down spin (right part) electrons. The relevant molecular orbitals are shown in figure 4 as isovalued surfaces. We also show the induced magnetic moments on all sites in figure 5 for some of the relevant systems. We will discuss the spectra, molecular orbitals and site distribution of the magnetic moments together. Let us note that the exchange splitting for carbon atom between spin up and spin down electron is ~ 2.49 eV. The magnetic moment is due to two up spin occupied orbitals, consistent with the Hund's rule. This brings the eigen values of atomic carbon p and zinc 4s quite close to each other for up states, while the down spin eigen value of carbon p is placed significantly higher. The formation of the spectra across the series reveals that the action is in the s-p complex formed by carbon p and zinc 4s orbitals, and the splitting of the up and down "bands" persists for all the systems, leading to the formation of the magnetic moment around carbon.

ZnC carries a magnetic moment of $\sim 2 \mu_B$ on carbon site. Because of the linear nature of ZnC , only one of the p orbitals is capable of hybridizing with Zn s. As a consequence triply degenerate p states (for the both the spins) split into two states as a singly degenerate and doubly degenerate once, retaining the exchange splitting between up and down. The corresponding molecular orbitals are shown in figure 4. A lowest state in the complex for both the spins are of similar nature and show significant hybridization and delocalization. The magnetic moment is due to the doubly degenerate pure p states localized on the carbon atom. The Mulliken population analysis shows effective charge transfer from Zn to C of order of ~ 1.7 electrons. Thus ignoring the splitting between up-down eigenvalues, a simple picture emerges. The charge transfer from zinc makes one of p orbitals on carbon doubly occupied. The delocalization caused by hybridization with 4s reduces Coulomb repulsion. The magnetic moment is due to the doubly degenerate pure p states localized on the carbon atom.

Next we turn to Zn_2C . Since in ZnC , two spin down orbitals on carbon are still unoccupied, one would naively expect Zn_2C to be nonmagnetic. Interestingly, Zn_2C also shows a magnetic moment of $\sim 2\mu_B$ mainly local-

TABLE I: The magnetic moment (μ_M) in μ_B , Exchange energy E_J (Energy difference between ferromagnetic and antiferromagnetic state) in meV, the nature of magnetic ground state for all the systems investigated.

Host Systems	Magnetic Moment μ_M		E_J (meV)	Nature of ground state	Geometry
	Singly doped	Doubly doped			
C	2	-	-	-	-
ZnO	2	-	-	-	Linear
Zn ₂ O ₂	2	0	-	AFM	Rhombous
Zn ₃ O ₃	2	0	-	AFM	Cap-triangle
Zn ₄ O ₄	2	4	-26.4	FM	Square
Zn ₅ O ₅	2	4	-3.3	FM	Ring
Zn ₆ O ₆	2	4	-2.5	FM	Ring
Zn ₇ O ₇	2	4	-1.1	FM	Ring
Zn ₇ O ₇ ^a	2	-	-	AFM	Ring
Zn ₈ O ₈	2	4	-0.9	FM	Two connected rings
Zn ₉ O ₉	2	4	-46.3	FM	3D
Zn ₁₀ O ₁₀	2	4	-26.3	FM	3D
Zn ₁₂ O ₁₂	2	4	-85.3	FM	3D
ZnO soild ^b	2	4	-89.3	FM	Wurtzite

^aZinc is nearest neighbour to both carbon atoms.

^bCalculation was performed on ZnO solid within large unit cell containing 72 atoms.

ized around the carbon atom. The hybridization of one of the p orbitals with two zinc 4s splits the spectrum of up and down electrons forming bonding and antibonding orbitals, the splitting being much less in the case of down electrons. As a consequence four up and two down orbitals are occupied. Once again by examining the molecular orbitals (figure 4), we arrived at a simple description namely; there are two doubly occupied orbitals which are delocalized (2p-4s hybridized). The magnetic moment arises out of two carbon based p's orbitals (homo-1 and homo-2 for up electrons). As a consequence of the hybridization a small but significant magnetic moment is induced on both zinc atoms.

Next we examine a typical motif Zn₂OC which brings in the role of oxygen. With introduction of oxygen, there is a competition between oxygen and carbon for charge transfer from zinc. The occupied molecular orbitals show interesting pattern. Evidently, relevant orbitals leading to magnetic interactions are homo and homo-1. The homo shows π bond formation between carbon and oxygen (homo perpendicular to plane) while homo-1 shows the σ bond. There are three down orbitals nearly compensating the charge in the three up orbitals. It can be seen that a significant magnetic moment ($\sim 0.42 \mu_B$) is induced on the oxygen sites, clearly because of homo and homo-1. The existence of π and σ bonds establishes the coupling between carbon and oxygen and is a crucial element in the formation of long range magnetic interactions even in the extended systems.

The ground state of symmetric cluster Zn₂C₂ is antiferromagnetic. There is a charge transfer of one electron

to carbon atoms from each of the zinc atoms. As a consequence the zinc-zinc distance increases by $\sim 0.2 \text{ \AA}$. As can be seen from figure 4, it is homo-2 which is responsible for antiferromagnetic coupling. This is analog of superexchange mechanism. It may be noted that a similar observation can be made for Zn₃OC₂ as well as for all the ring clusters when carbon atoms are placed on both sides of zinc atom. We recall that the experiment indicate a saturation of magnetic moment per carbon atom around 5 % substitution.

Now, we turn our attention to ring structures Zn₅O₅ – Zn₇O₇. We discuss the typical case of Zn₇O₅C₂ showing the ferromagnetic behaviour. The relevant molecular orbitals are shown in figure 6. In this case two carbon atoms are separated by chain of zinc-oxygen-zinc (see figure 5). It can be seen from alpha homo and alpha homo-1, that there is a π bond formation between three p orbitals centered on two carbon atoms and one oxygen atom. A similar bonding is also seen in alpha homo-2 and alpha homo-3 as well as in beta orbitals which are shown in figure 6. These are the orbitals which are responsible for the ferromagnetic interaction between the carbon atoms mediated via oxygen.

Zn₁₂O₁₀C₂ is a three dimensional structure. As pointed out earlier when the structure changes to three dimensional one, there is a significant change in the connectivity of two carbon atoms via zinc and oxygen. The ground state structure for this system is shown in figure 2. The induced magnetic moments are shown in figure 5. It can be seen that the induced magnetic moments on two nearest neighbor oxygen sites are substantial $\sim 0.180 \mu_B$.

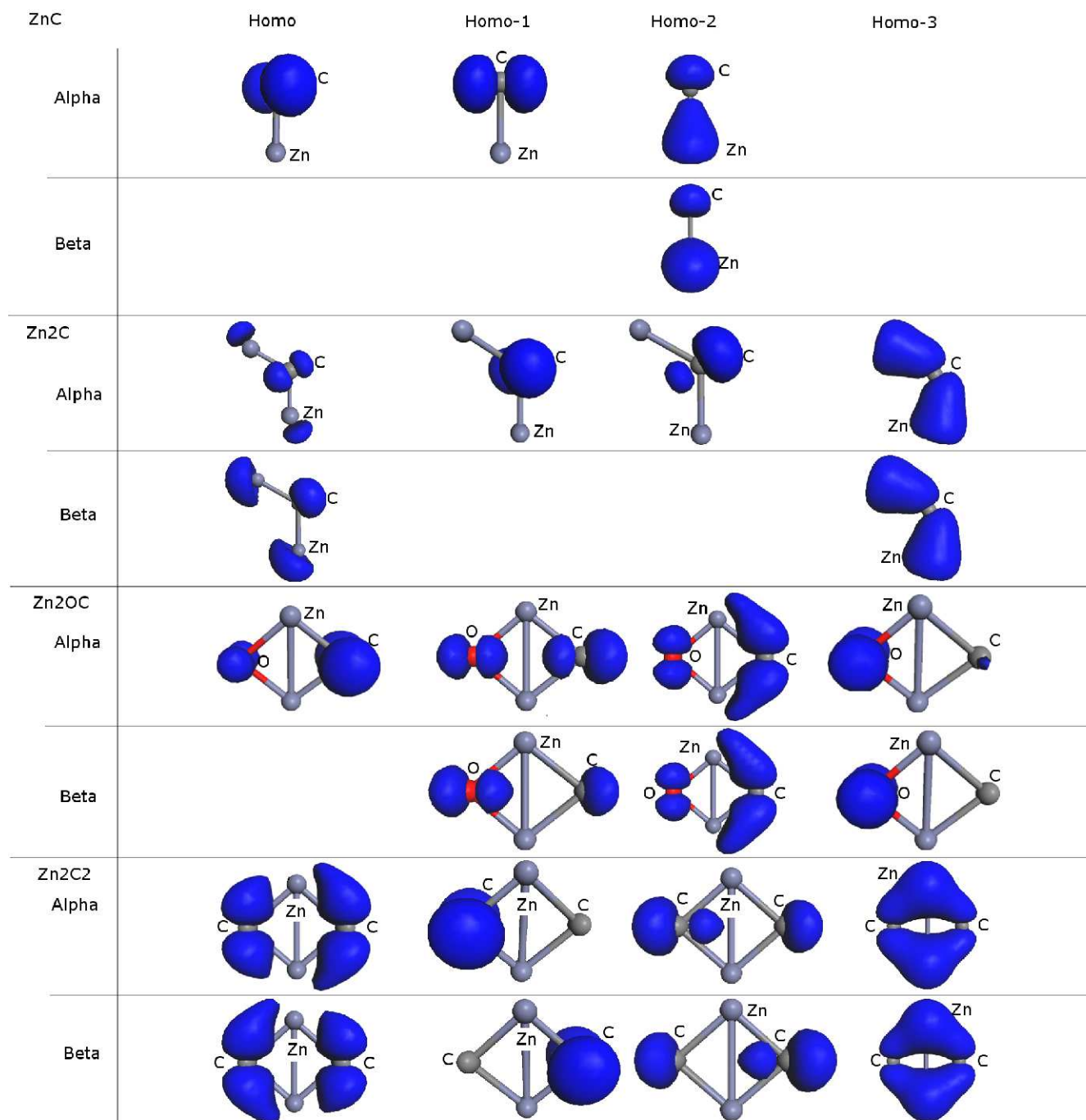


FIG. 4: Isovalued surfaces of molecular orbitals for up(alpha) and down(beta) electrons. The position of substituted carbon is marked by C.

Other oxygen sites connecting them also have notable magnetic moments. The relevant molecular orbitals (alpha homo - alpha homo-2) and the spin density are shown in figure 7. Clearly the picture described in the earlier cases continues in the present case. The induced spin density shows the magnetic moment on carbon and oxygen sites. These homos show interaction between two

carbon atoms mediated via oxygen. Thus, in these case once again the magnetic interaction between the carbon atoms is mediated via p orbitals (π -bond). The most significant point is that the interaction is strengthened by availability of multiple sites connecting two carbon atoms. In this case, the C-C distance is $\sim 5.410 \text{ \AA}$.

We expect a similar picture to be valid in ZnO solid.

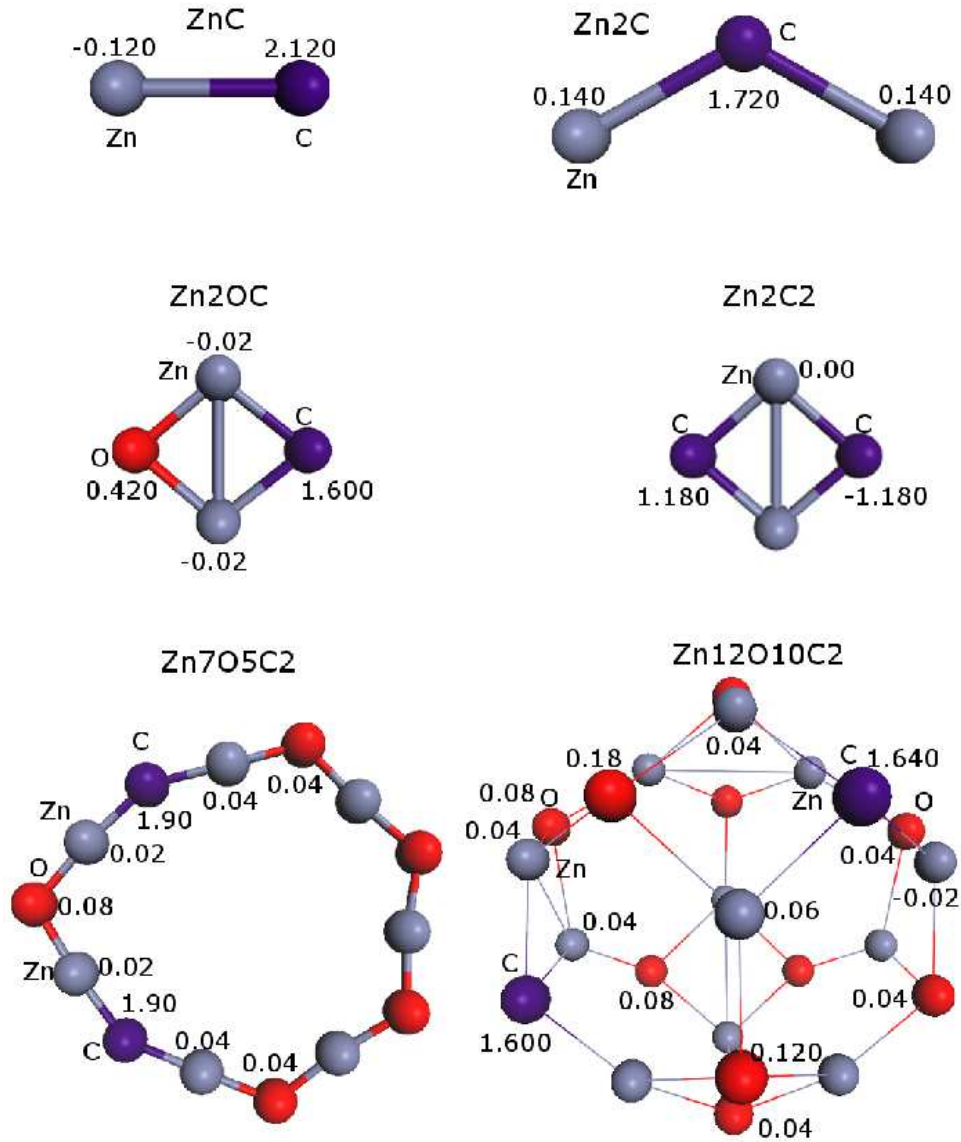


FIG. 5: Spin moment at site is depicted in C-doped clusters. The position of substituted carbon is marked as C.

We have considered a large unit cell with 72 atoms containing two carbon atoms separated by 7.6 \AA . Our results for the density of states (DOS) and magnetic moments are consistent with the report of Pan et.al.¹³ We find that the spin-up bands are fully occupied while the spin-down bands are partially filled resulting in the magnetic moment of $\sim 2\mu_B$ per carbon atom. We show the relevant molecular orbitals near the top of the valence band for up electrons. It can be noted from figure 8 that the two carbon atoms are separated by a zinc oxide plane. We also show the spin density in figure 9. The molecular orbitals depict two different ways in which the interaction is mediated. In the case of alpha-1, the carbon (in the top plane) induces magnetic moments on oxygen sites within the plane which then couples to the oxygen in the bottom plane as seen in figure 8. In the case of orbitals marked

as alpha-2, the carbon induces the magnetic moments in the plane, below and above which couples the carbon site in the bottom plane. These figures clearly bring out the role of the three-dimensional oxygen network in providing the multiple paths between two carbon atoms. The resulting spin density is shown in figure 9. As expected, the spin density is positive and is mainly around carbon sites. The induced magnetic moments on oxygen sites are clearly seen.

IV. SUMMARY AND CONCLUDING REMARKS

We have carried out spin-polarized electronic structure calculations on a series of $(\text{ZnO})_n$ and the substitutionally

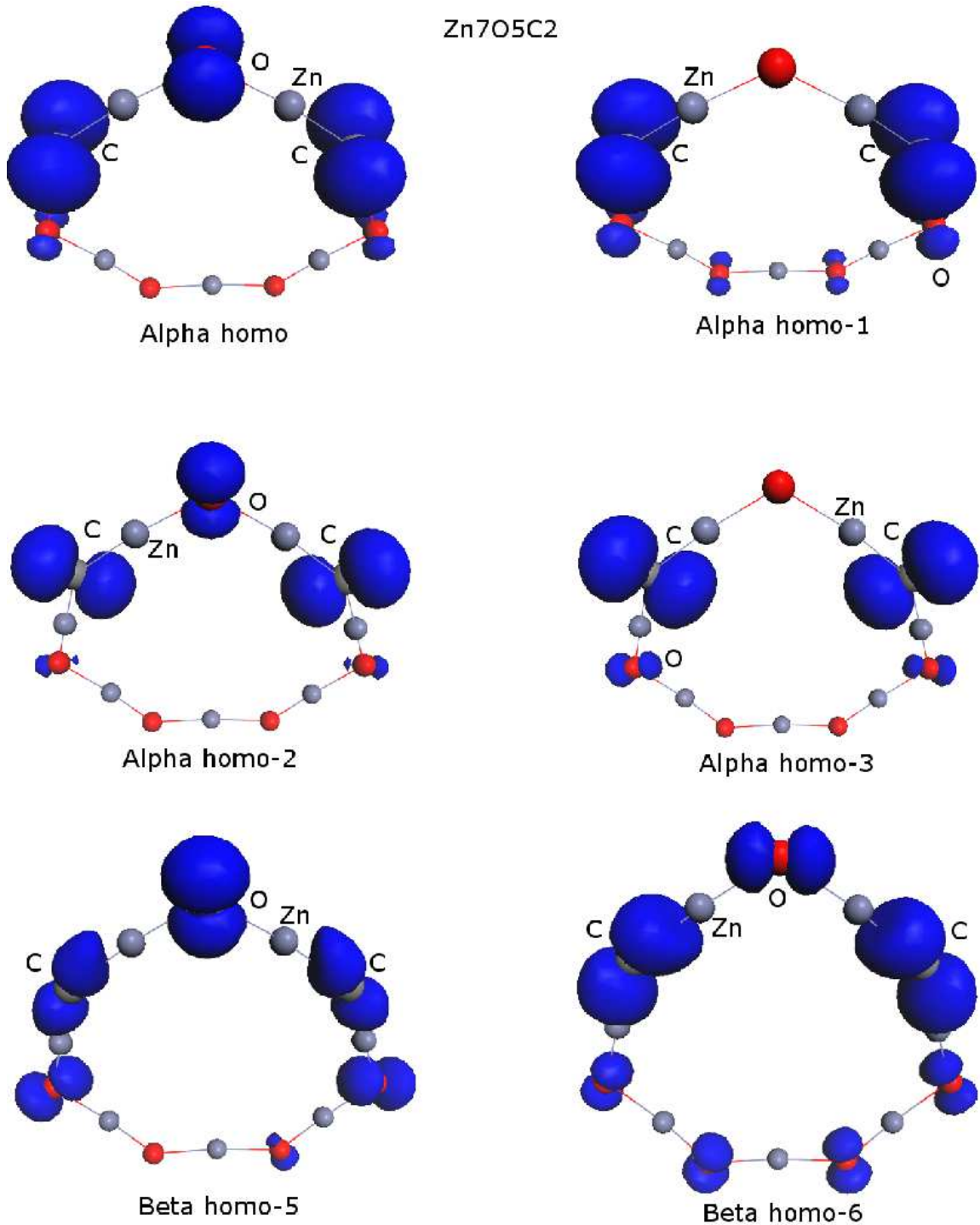


FIG. 6: Isovalued surfaces of molecular orbitals for up and down electrons in C-doped Zn₇O₇ clusters. The oxygen atoms are indicated by red color (online) whereas the position of substituted carbon is marked by C.

doped Zn_nO_{n-m}C_m clusters with $n = 1 - 10, 12$ and $m = 1 - 2$ as well as for zinc oxide solid with a view to elucidate the origin of magnetism in carbon doped zinc oxide. Our calculations reveal the crucial role played by oxygen in mediating ferromagnetic interaction. A detailed study of molecular orbitals show that the inter-

action is mediated via π as well σ bonds (especially in three dimensional solid) formed out of p electrons of carbon and oxygen. Our calculations also bring out the role played by hybridization of zinc 4s with carbon 2p and oxygen 2p. We expect the antiferromagnetic coupling if carbon atoms get substituted on sites adjacent to zinc

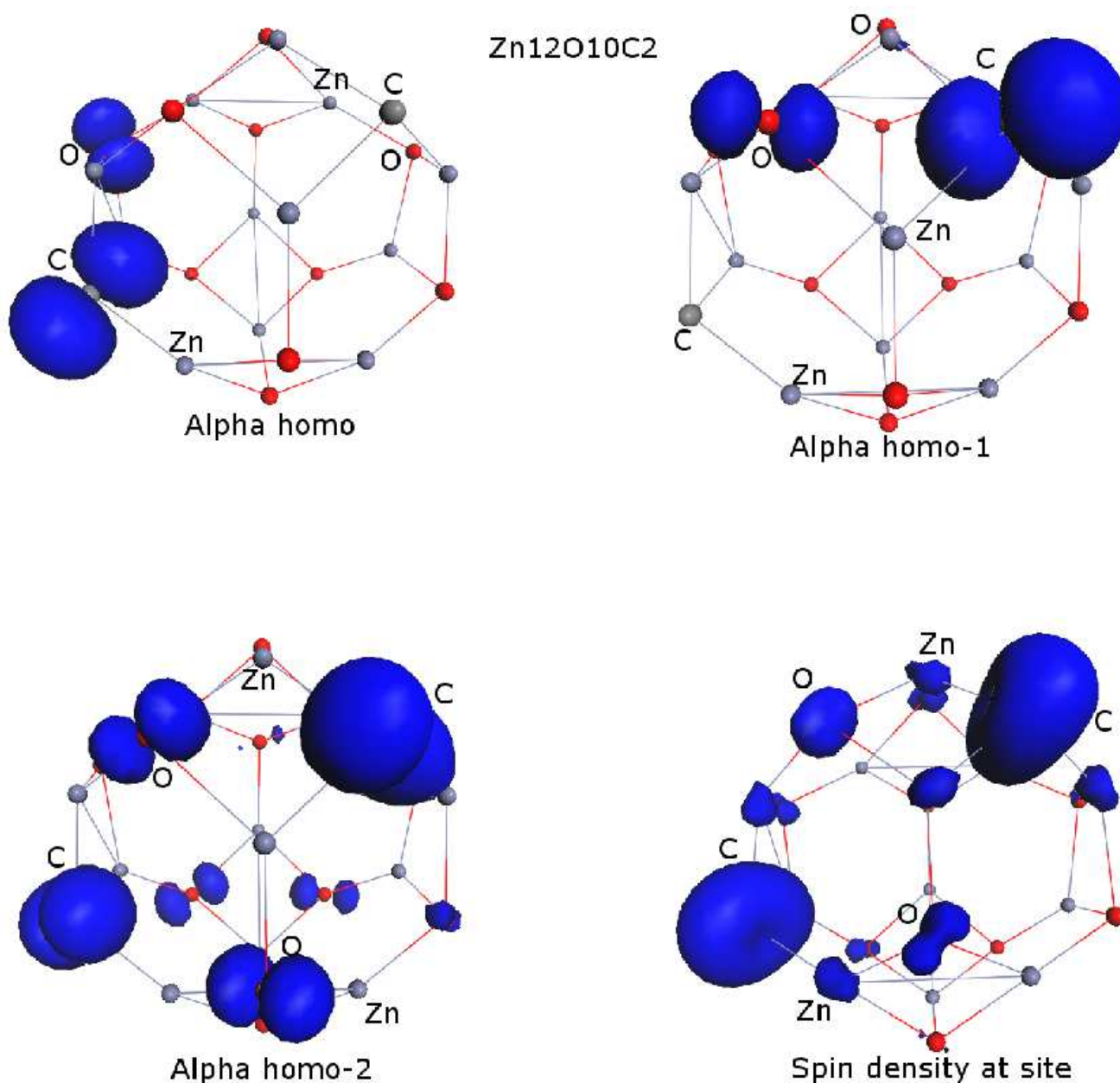


FIG. 7: Isovalued surfaces of molecular orbitals for up and down electrons in C-doped $Zn_{12}O_{12}$ clusters. The isosurface spin density at site is also shown. The position of substituted carbon is marked by C.

leading to saturation of magnetic moment with increasing carbon content. The results clearly show a significant enhancement in the ferromagnetic interaction between the two carbon atoms due to higher dimensionality, bringing out the role of multiple connectivity (between two carbon atoms) of the Zn-O network.

Acknowledgments

We are grateful to Accelrys Inc. USA for providing us the demonstration version of CASTEP. We also thanks to

CDAC, India for providing us the high performance computing facility. B. J. Nagare thanks to Balchandra Pujari and Vaibhav Kaware for their help during the project.

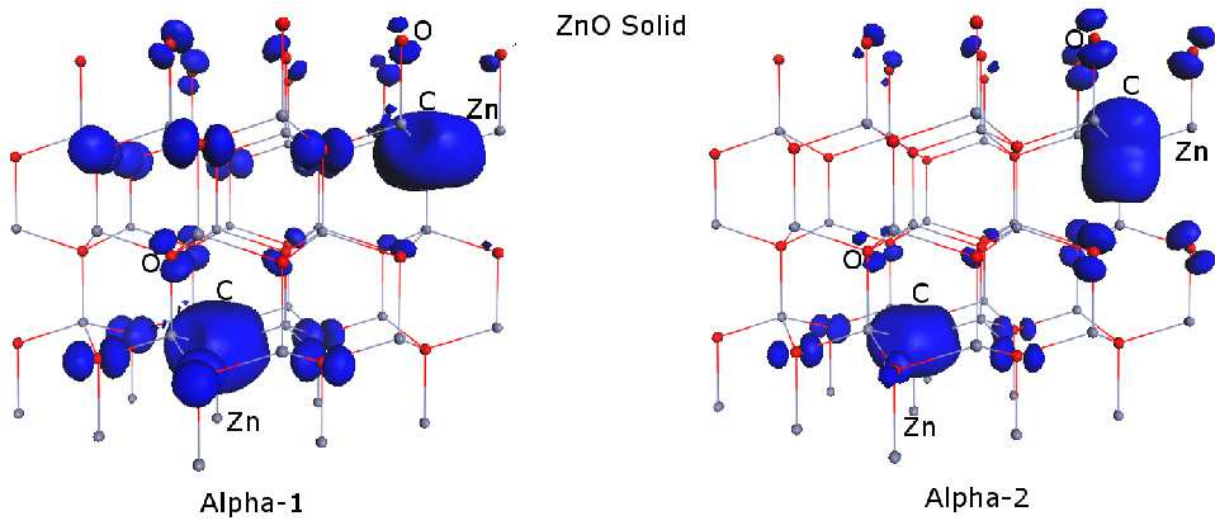


FIG. 8: Isovalued surfaces of molecular orbitals in C-doped zinc oxide solid for up electrons at the top of the valence band. The position of substituted carbon is marked as C.

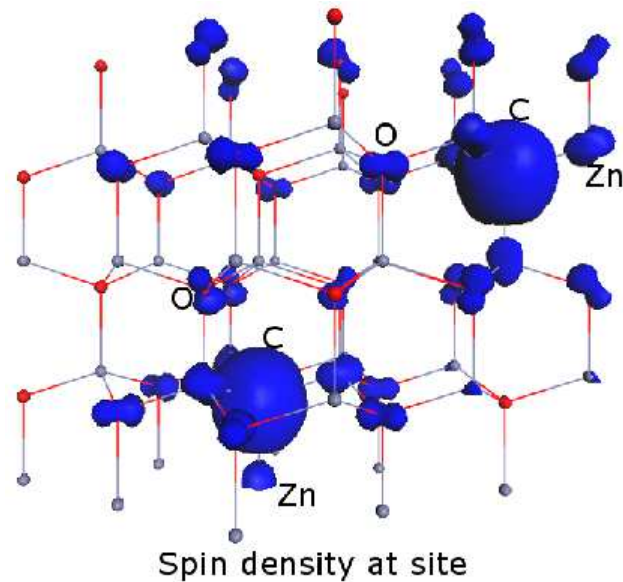


FIG. 9: The isosurface spin density at site is shown for the case of C-doped zinc oxide solid. The position of substituted carbon is marked as C.

* Electronic address: bjnagare@physics.mu.ac.in

† Electronic address: sajeev.chacko@gmail.com

‡ Electronic address: kanhere@unipune.ernet.in

¹ J. M. D. Coey, M. Venkatesh, and C. B. Fitzgerald, *Nat. Mater.* **4**, 173 (2005).

² N. H. Hong, J. Sakai, N. Poirot, and Ruyter, *Appl. Phys. Lett.* **86**, 242505 (2005).

³ J. He, S. Xu, Y. K. Yoo, Q. Xue, H. C. Lee, S. Cheng, X. Xiang, G. Dionne, and I. Takeuchi, *Appl. Phys. Lett.* **86**, 052503 (2005).

⁴ N. H. Hong, J. Sakai, W. Prellier, and G. F. A. Hassini, *Phys. Rev. B* **72**, 045336 (2005).

⁵ M. Venkatesh, C. B. Fitzgerald, J. G. Lunney, and J. M. D. Coey, *Phys. Rev. Lett.* **93**, 177206 (2004).

⁶ Y. Lin-Hui, A. J. Freeman, and B. Delley, *Phys. Rev. B* **73**, 033203 (2006).

⁷ D. B. Buchholz, R. P. H. Chang, J. H. Song, and J. B. Ketterson, *Appl. Phys. Lett.* **87**, 082504 (2005).

⁸ N. Sanchez, S. Gallego, and M. Munoz, *Phys. Rev. Lett.* **101**, 067206 (2008).

- ⁹ A. Walsh, J. L. F. D. Silva, and S.-H. Wei, Phys. Rev. Lett. **100**, 256401 (2008).
- ¹⁰ A. J. Behan, A. Mokhtari, H. J. Blythe, D. Score, X.-H. Xu, J. R. Neal, A. M. Fox, and G. A. Gehring, Phys. Rev. Lett. **100**, 047206 (2008).
- ¹¹ Q. Wang, Q. Sun, G. Chen, Y. Kawazoe, and P. Jena, Phys. Rev. B **74**, 205411 (2008).
- ¹² A. R. Botello-Méndez, F. López-Urías, M. Terrones, and H. Terrones, Nano Letters. **8**, 1562 (2008).
- ¹³ H. Pan, J. B. Yi, L. Shen, R. Q. Wu, J. H. Yang, J. Y. Lin, J. Ding, L. H. Van, and J. H. Yin, Phys. Rev. Lett. **99**, 127201 (2007).
- ¹⁴ D. Vanderbilt, Phys. Rev. B **41**, 7892 (1990).
- ¹⁵ S. J. Clark, M. D. Segall, C. J. Pickard, P. J. Hasnip, M. J. Probert, K. Refson, and M. C. Payne, Zeitschrift fuer Kristallographie. **220(5-6)**, 567 (2005).
- ¹⁶ G. Kresse and D. Joubert, Phys. Rev. B **59**, 1758 (1999).
- ¹⁷ J. P. Perdew, K. Burke, and M. Ernzerhof, Phys. Rev. Lett. **77**, 3865 (1996).
- ¹⁸ J. M. Matxain, J. E. Fowler, and J. M. Ugalde, Phys. Rev. A **62**, 053201 (2000).
- ¹⁹ G. L. Gustev, B. K. Rao, and P. Jena, J. Phys. Chem. A **104**, 5374 (2000).
- ²⁰ J. E. Jaffe, Snyder, J. A. Lin, and A. C. Z. Hess, Phys. Rev. B **62**, 1660 (2000).